Structural and Functional Consequences of Substitutions at the Tyrosine 55−Lysine 104 Hydrogen Bond in *Escherichia coli* Inorganic Pyrophosphatase[†]

Igor P. Fabrichniy,[‡] Vladimir N. Kasho,[§] Teppo Hyytiä,[||] Tiina Salminen,[⊥,▽] Pasi Halonen,[||] Valeriy Yu. Dudarenkov,[‡] Pirkko Heikinheimo,[⊥,▽] Victor Ya. Chernyak,[‡] Adrian Goldman,[⊥,▽] Reijo Lahti,[⊥] Barry S. Cooperman,*[,§] and Alexander A. Baykov*[,‡]

A. N. Belozersky Institute of Physico-Chemical Biology and School of Chemistry, Moscow State University, Moscow 119899, Russia, Center for Ulcer Research and Education, Department of Medicine, University of California, Los Angeles, California 90073, Department of Chemistry, University of Pennsylvania, Philadelphia, Pennsylvania 19104-6323, Department of Biochemistry, University of Turku, FIN-20500 Turku, Finland, and Centre for Biotechnology, FIN-20251 Turku, Finland

Received December 5, 1996; Revised Manuscript Received March 18, 1997[⊗]

ABSTRACT: Tyrosine 55 and lysine 104 are evolutionarily conserved residues that form a hydrogen bond in the active site of *Escherichia coli* inorganic pyrophosphatase (E-PPase). Here we used site-directed mutagenesis to examine their roles in structure stabilization and catalysis. Though these residues are not part of the subunit interface, Y55F and K104R (but not K104I) substitutions markedly destabilize the hexameric structure, allowing dissociation into active trimers on dilution. A K104I variant is nearly inactive while Y55F and K104R variants exhibit appreciable activity and require greater concentrations of Mg^{2+} and higher pH for maximal activity. The effects on activity are explained by (a) increased pK_as for the catalytically essential base and acid at the active site, (b) decreases in the rate constant for substrate (dimagnesium pyrophosphate) binding to enzyme−Mg_2 complex vs enzyme−Mg_3 complex, and (c) parallel decreases in the catalytic constant for the resulting enzyme−Mg_2−substrate and enzyme−Mg_3−substrate complexes. The results are consistent with the major structural roles of Tyr55 and Lys104 in the active site. The microscopic rate constant for PP_i hydrolysis on either the Y55F or K104R variants increases, by a factor of 3−4 in the pH range 7.2−8.0, supporting the hypothesis that this reaction step depends on an essential base within the enzyme active site.

Inorganic pyrophosphatase (EC 3.6.1.1; PPase)[1] belongs to a group of enzymes catalyzing phosphoryl transfer from phosphoric acid anhydrides to water, a principal reaction of cell bioenergetics. Soluble PPases hydrolyze PP_i to P_i with release of energy as heat and provide in this way a thermodynamic pull for many biosynthetic reactions (Kornberg, 1962), while membrane-bound PPases utilize this energy for transmembrane H^+ transport (Baltscheffsky & Baltscheffsky, 1992; Rea & Poole, 1993). PPases have been shown to be essential in bacteria (Chen et al., 1990), yeast (Lundin et al., 1991), and plants (Sonnewald, 1992).

Reactions catalyzed by PPase include PP_i hydrolysis, PP_i synthesis, and P_i−H_2O oxygen exchange, and all require divalent metal ions, with Mg^{2+} conferring the highest activity. A total of three to five Mg^{2+} ions per active site are required for the activity of *Escherichia coli* PPase (E-PPase; Baykov et al., 1990, 1996; Käpylä et al., 1995). Catalysis proceeds without formation of phosphorylated enzyme (Gonzalez et al., 1984) (Scheme 1).

Scheme 1: PP_i−P_i Equilibration by PPase[a]

$$EM_{n-2} \underset{k_2}{\overset{k_1}{\rightleftharpoons}} EM_nPP_i \underset{k_4}{\overset{k_3}{\rightleftharpoons}} EM_n(P_i)_2 \underset{k_6}{\overset{k_5}{\rightleftharpoons}} EM_{n-1}P_i + MP_i \underset{k_8}{\overset{k_7}{\rightleftharpoons}} EM_{n-2}$$

[a] $K_1 = k_1/k_2$, $K_3 = k_3/k_4$, $K_5 = k_5/k_6$, $K_7 = k_7/k_8$, $n = 3-5$.

E-PPase is hexameric, and its structure, recently determined to a resolution of 2.2 Å (Harutyunyan et al., 1996b; Kankare et al., 1996a,b), is best described as a dimer of two trimers. Recent work from these groups has concentrated on determining the consequences of active-site mutation on both quaternary structure and enzyme mechanism (Käpylä et al., 1995; Baykov et al., 1995; Volk et al., 1996). Here we extend these studies to two conserved active-site residues, Tyr55 and Lys104, the side chains of which form a hydrogen bond within the active site (Kankare et al., 1996a,b; Harutyunyan et al., 1996b).

The active site is present in each monomeric unit of E-PPase and contains 14 polar amino acid residues that are completely conserved in all known soluble PPases, despite only moderate sequence similarity of the rest of the molecule (Cooperman et al., 1992). Furthermore, for the three PPases whose crystal structures have been determined, i.e., those from *E. coli*, *Thermus thermophilus* (Teplyakov et al., 1994), and *Saccharomyces cerevisiae* (Heikinheimo et al., 1996;

[†] This work was supported by grants from NIH (DK13212 and TW00407), the Finnish Academy of Sciences (Grants 1444, 3875, and 4310), the Russian Foundation for Basic Research (94-04-12658), and the Russian State Project Bioengineering, section Enzyme Engineering (1-42).

* Authors to whom to address correspondence (B.S.C. FAX 215-898-2037, telephone 215-898-6330, email cooprman@pobox.upenn.edu; A.A.B. FAX 095-939-3181, telephone 095-939-5541, email abaykov@protchem.genebee.msu.su).

[‡] Moscow State University.

[§] University of California.

[||] University of Pennsylvania.

[⊥] University of Turku.

[▽] Centre for Biotechnology.

[⊗] Abstract published in *Advance ACS Abstracts,* June 1, 1997.

[1] Abbreviations: E-PPase, *Escherichia coli* inorganic pyrophosphatase; P_i, inorganic phosphate; PPase, inorganic pyrophosphatase; PP_i, inorganic pyrophosphate; WT, wild type.

S0006-2960(96)02984-4 CCC: $14.00

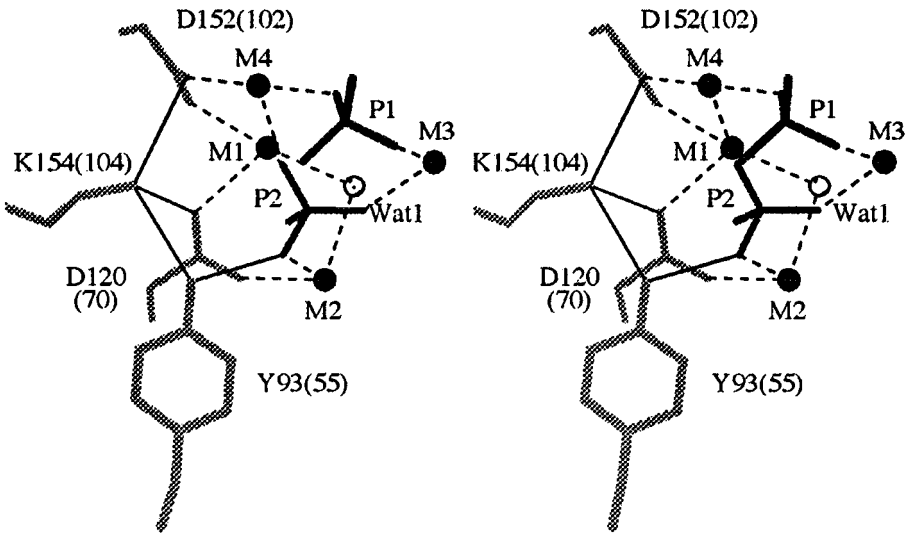

FIGURE 1: Stereo diagram showing the positions of Tyr93 and Lys154 with respect to two phosphate (P1 and P2) and four manganese ions (M1−M4) in the active site of *S. cerevisiae* PPase (Heikinheimo et al., 1996). Wat1 is a water molecule shared by M1 and M2. Numbering in parentheses refers to *E. coli* PPase.

Harutyunyan et al., 1996a), the detailed structures of the active site are highly conserved. As a result, the structure of the product complex *S. cerevisiae* PPase−$Mn_4(P_i)_2$ is pertinent to our present studies on E-PPase variants (as yet, no substrate or product complex structures of E-PPase have been determined). Most significantly, this structure identifies four divalent metal ion binding subsites (M1−M4) and two phosphate binding subsites (P1 and P2) within the active site, with subsite P1 corresponding to the higher affinity subsite and P2 to the lower affinity subsite. All four subsites M1−M4 interact directly with P2, but only M3 and M4 interact with P1. As can be seen (Figure 1), Tyr55 forms a direct hydrogen bond to P2, and both Tyr55 and Lys104 are important in positioning Asp70 so that it can coordinate M1 and M2. These two metal ions, in turn, bind to Wat1, aiding in its deprotonation and thereby activating it as the nucleophile required for PP_i hydrolysis (Heikinheimo et al, 1996). In addition, Tyr55 is part of a hydrophobic cluster with residues in helix A of E-PPase (Phe137, Phe138, and Tyr141) that forms an important part of the trimer−trimer interface (Kankare *et al.*, 1996a).

Our results demonstrate the importance of Tyr55 for hexamer stability and of both Lys104 and Tyr55 for substrate/product binding and PP_i hydrolysis, indicate the highly integrated nature of the active site, and provide strong support for the hypothesis (Salminen et al., 1995; Heikinheimo et al., 1996) that hydrolysis of enzyme-bound PP_i (rate constant k_3) depends upon an essential base.

EXPERIMENTAL PROCEDURES

Enzymes. Wild type-free variant PPases were expressed and purified using the overproducing *E. coli* strain MC1061/*YPPAI*(Δ*ppa*) (Salminen *et al*., 1995). Stock PPase solutions, except as noted, were made up in 0.1 M Tris/HCl buffer (pH 7.2) containing 20 mM $MgCl_2$ and 50 μM EGTA and were preincubated for at least 1 h at the indicated temperature before use. Trimeric PPase was prepared by incubating 5 μM enzyme for 15 h at 0 °C in 0.15 M Tris/HCl buffer (pH 8.5) containing 1 mM Mg^{2+} and 40 μM EGTA. Enzyme concentration was estimated on the basis of a subunit molecular mass of 20 kDa (Josse, 1966) and an $A_{280}^{1\%}$ of 11.8 (Wong *et al.*, 1970).

Methods. Procedures used to measure enzyme-catalyzed rates of PP_i hydrolysis, PP_i synthesis, oxygen exchange, and Mg^{2+} binding to PPase were as described previously (Baykov et al., 1996; Volk et al., 1996). Sedimentation velocity measurements were performed in the presence of 1 mM $MgCl_2$, using 5−7.5 μM enzyme preequilibrated for 2 h at 20−25 °C or for 14 h at 4 °C (Volk et al., 1996). Enzyme-bound PP_i was assayed by a modified coupled enzyme procedure (Nyrén & Lundin, 1985; Baykov et al., 1990). Equilibrated reaction mixtures (50 μL) containing enzyme, P_i, $MgCl_2$, buffer, and EGTA were quenched with 10 μL of 5 M trifluoroacetic acid, kept for 3−5 min at room temperature, and centrifuged for 1 min at 5000*g*. A 5-μL aliquot of the supernatant was added to 0.3 mL of the PP_i assay cocktail, and the resulting luminescence was recorded with an LKB Model 1250 luminometer. After the line stabilized, 5 μL of 10 μM PP_i solution was added to calibrate the assay. The PP_i assay cocktail was prepared by mixing 6 mL of 0.2 M Tris/HCl buffer (pH 8.0) containing 1 mM dithiothreiotol, 0.8 mg/mL bovine serum albumin, and 30 μM EGTA, with 40 μL of 67 units/mL ATP-sulfurylase solution (Sigma lyophilized preparation reconstituted with water), 200 μL of luciferin/luciferase solution (Sigma ATP assay mix, catalog no. FL-ASC, reconstituted with 5 mL of water), and 60 μL of 1 mM adenosine 5′-phosphosulfate (Sigma). A radioisotopic procedure (Springs et al., 1981) gave essentially the same amounts of enzyme-bound PP_i.

The following buffers were used for measurement of steady-state rates of PP_i hydrolysis, net PP_i synthesis, and P_i−H_2O oxygen exchange and of enzyme-bound PP_i formation: 0.15−0.20 M Tris/HCl (pH 7.2), 0.25−0.30 M Tris/HCl (pH 8.0), 0.21 M 2-amino-2-methyl-1-propanol/HCl (pH 9.3), and 0.45−0.60 M 2-amino-2-methyl-1-propanol/HCl (pH 10.0). All buffers contained EGTA, 40 μM (pH 7.2 and 8.0), or 1 μM (pH 9.3 and 10). All experiments were performed at 25 °C, except as noted.

Calculations and Data Analysis: (A) Hexamer−Trimer Equilibration. Equations 1 and 2 describe time courses of activity (*A*) resulting from hexamer (E_6) dissociation into trimers (E_3) and trimer association into hexamers (Scheme 2) and, at $t = \infty$ ($d\alpha_H/dt = 0$), the equilibrium activity as a function of enzyme concentration. A_H and A_T are specific

activities of hexamer and trimer, respectively, α_H is the fraction of enzyme in the hexameric form at time t, $[E]_t$ is total enzyme concentration, expressed in monomers, and k_a and k_d are the rate constants for hexamer formation and breakdown. Equations 1 and 2 were fit to data with the program SCIENTIST (MicroMath).

Scheme 2: Hexamer−Trimer Equilibrium

$$E_6 \underset{k_a}{\overset{k_d}{\rightleftharpoons}} 2E_3$$

$$A = A_T + (A_H - A_T)\alpha_H \quad (1)$$

$$\frac{d\alpha_H}{dt} = \frac{2}{3}k_a[E]_t(1 - \alpha_H)^2 - k_d\alpha_H \quad (2)$$

(B) Mg_2PP_i Hydrolysis. The apparent catalytic constant k_h as well as the apparent Michaelis constant $K_{m,h}$ for PPase catalysis of Mg_2PP_i hydrolysis was determined as a function of $[Mg^{2+}]$ and pH. Fitting k_h to eq 3, derived from Scheme 3 (Volk et al., 1996), allowed evaluation of $k_h^{(2)}$ and $k_h^{(3)}$, the catalytic constants for HM_2ES and HM_3ES, respectively, as well as the dissociation constants K'_{ESH2}, K'_{ESH}, K_{ESH2}, K^{H2}_{a3}, and K^{H}_{a3} for the corresponding equilibria in Scheme 3.

Scheme 3: Equilibria Linking Stoichiometrically Significant Species within Enzyme−Substrate Complex

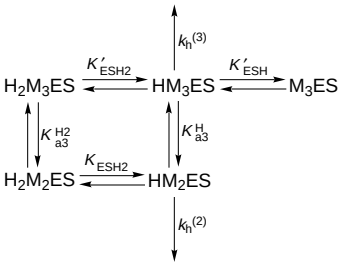

$$k_h = \frac{k_h^{(3)} + k_h^{(2)}K^{H}_{a3}/[Mg^{2+}]}{1 + K^{H}_{a3}/[Mg^{2+}] + [H^+]/K'_{ESH2}(1 + K^{H2}_{a3}/[Mg^{2+}]) + K'_{ESH}/[H^+]} \quad (3)$$

(C) PP_i−P_i Equilibration. The eight rate constants in Scheme 1, k_1−k_8, were evaluated at a given pH and $[Mg^{2+}]$ as described earlier (Springs et al., 1981; Smirnova et al., 1995). Values for K_3, K_5, and K_7 were determined by fitting the dependence on $[MgP_i]$ of f_{epp}, the fraction of total enzyme containing bound PP_i, to

$$f_{epp} = 1/\Sigma \quad (4)$$

where $\Sigma = 1 + K_3 + K_3K_5/[MgP_i] + K_3K_5K_7/[MgP_i]^2$.

With these equilibrium constants known, values for the eight rate constants could be evaluated from measurements of k_h and $k_h/K_{m,h}$, of the rates of oxygen exchange (v_{ex}) and net PP_i synthesis (v_s), and of the partition coefficient, P_c, which defines the probability of enzyme-bound P_i undergoing oxygen exchange with water vs being released into solution (Hackney & Boyer, 1978). P_c was calculated from the distribution of all ^{18}O-labeled forms of P_i according to Hackney (1980). The relevant equations follow.

$$k_5 = v_{ex}\Sigma(1 - 0.75P_c)/P_c\,K_3[E]_t \quad (5)$$

$$k_6 = k_5/K_5 \quad (6)$$

$$k_4 = k_5\,P_c/(1 - P_c) \quad (7)$$

$$k_3 = k_4K_3 \quad (8)$$

$$k_7 = 1/(1/k_h - 1/k_3 - 1/k_5 - k_4/k_3k_5) \quad (9)$$

$$k_8 = k_7/K_7 \quad (10)$$

$$k_1 = (1 + k_2/k_3 + k_2k_4/k_3k_5)\,k_h/K_{m,h} \quad (11)$$

$$k_2 = v_s\Sigma\,(k_3 + k_4)/([E]_t\{k_3 + k_4\} - v_s\Sigma) \quad (12)$$

At combinations of pH and $[Mg^{2+}]$ where it was not feasible to achieve saturating concentrations of $[MgP_i]$, values for k_1−k_3 could be estimated from measurements of v_{ex}, v_s, f_{epp}, and P_c performed at a nonsaturating $[MgP_i]$, employing eqs 13−15.

$$k_3 = \frac{v_{ex}(1 - 0.75\,P_c)}{[E]_t\,f_{epp}(1 - P_c)} \quad (13)$$

$$\frac{v_s/[E]_t}{f_{epp}} < k_2 < \frac{v_s/[E]_t}{f_{epp} - v_s/[E]_tk_3} \quad (14)$$

$$k_1 = k_h/K_{m,h}\,\{1 + k_2/[k_3(1 - P_c)]\} \quad (15)$$

RESULTS

Dissociation of Y55F and K104R PPase into Trimers. Previously we showed that Y55F and K104R substitutions increased Nile Red binding and electrophoretic mobility of *E. coli* PPase, suggesting a change in enzyme quaternary structure (Lahti et al., 1990a,b; Salminen et al., 1995). This suggestion was confirmed in the present work by sedimentation measurements. The value of the sedimentation coefficient, $s_{20,w}$, for Y55F PPase (pH 7.2−9.5) and K104R PPase (pH 6.5−8.5) was 6.4 ± 0.2 S at 20−25 °C, i.e., close to that for WT PPase, but dropped to 3.9 ± 0.2 and 4.2 ± 0.2 S, respectively, at 4 °C (pH 8.5). The molecular mass of Y55F PPase estimated from sedimentation equilibrium at 4 °C was 58 ± 6 kDa, indicating that the enzyme is predominantly trimeric under the conditions used (8 μM enzyme and 1 mM $MgCl_2$, pH 8.5). By contrast, K104I PPase, like WT PPase (Velichko et al., 1995), retained the value of $s_{20,w}$ of 6.3 ± 0.2 S at 4 °C (pH 8.5), indicating no change in quaternary structure, consistent with our observation that the electrophoretic mobilities of K104I PPase and WT PPase are identical (Salminen et al., 1995). Thus, for this variant, the observed changes in Nile Red binding, vis-à-vis wild-type enzyme (Salminen et al., 1995) are not associated with hexamer dissociation.

The specific activities of Y55F and K104R PPase depend markedly on enzyme concentration in the stock solution (Figure 2), consistent with lower activity of trimer in the assay conditions (see also below). The data in Figure 2 show that the Y55F hexamer is much more destabilized than the K104R hexamer. The Y55F and K104R hexamers are stabilized by raising the temperature from 0 to 25 °C, as

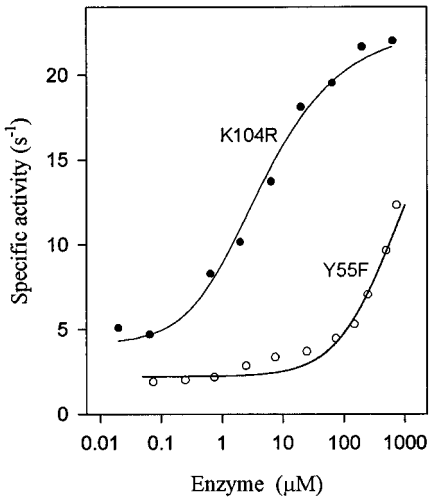

FIGURE 2: Specific activities of Y55F and K104R PPase preequilibrated at different enzyme concentrations. Following overnight incubation at 0 °C in the presence of 1 mM $MgCl_2$ and 0.15 M Tris/HCl, pH 8.5, enzyme activity was assayed at 25 °C in the presence of 20 μM PP_i, 20 mM $MgCl_2$, and 0.15 M Tris/HCl, pH 9.0. The lines are drawn to eqs 1 and 2 by setting $t = \infty$ and using K_d values shown in Table 1.

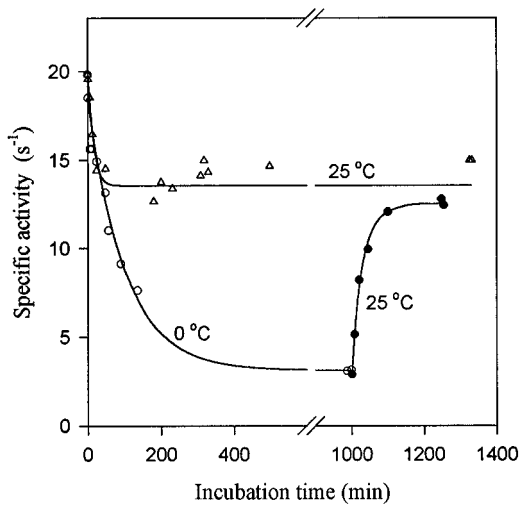

FIGURE 3: Reversibility of the cold-induced inactivation of Y55F PPase. Stock enzyme solution (50 μM) preequilibrated at 25 °C was diluted to 0.15 μM into 0.15 M Tris/HCl buffer, pH 8.5, and incubated at 25 °C (triangles) or 0 °C (open circles); in 16.7 h, the temperature of the second incubation was raised to 25 °C (closed circles). Enzyme activity was assayed at 25 °C in the presence of 20 μM PP_i, 20 mM $MgCl_2$, and 0.15 M Tris/HCl, pH 9.0. The lines are drawn to eqs 1 and 2, using parameter values shown in Table 1.

Table 1: Rate and Equilibrium Constants for Hexamer−Trimer Equilibration[a]

temperature (°C)	K_d (μM)	k_d (h^{-1})	k_a ($\mu M^{-1}\ h^{-1}$)
	Y55F PPase		
25	0.015 ± 0.006	0.33 ± 0.15[b]	22 ± 1
0	370 ± 40	0.60 ± 0.05	0.0016 ± 0.0003[c]
	K104R PPase		
25	0.022 ± 0.006	1.4 ± 0.6[b]	65 ± 9
0	1.5 ± 0.2	0.7 ± 0.2	0.5 ± 0.2[c]

[a] Measured at pH 8.5 in the presence of 1 mM $MgCl_2$. [b] Calculated as k_aK_d. [c] Calculated as k_d/K_d.

Table 2: Dissociation Constants for Mg^{2+} Binding to PPase Determined by Equilibrium Dialysis[a]

pH	K_{m1} (mM)	K_{m2} (mM)	K_{m3} (mM)
	Y55E PPase		
7.2	0.084 ± 0.009 (0.080)	1.6 ± 0.3 (1.74)	
8	0.093 ± 0.008 (0.054[b])	2.4 ± 0.6 (2.1[b])	
9.3	0.025 ± 0.002 (0.016)	0.75 ± 0.11 (0.34)	1.1 ± 0.2 (1.3)
	K104R PPase		
7.2	0.112± 0.008	2.0 ± 0.3	
8	0.13 ± 0.01	3.8 ± 0.4	
9.3	0.041 ± 0.002	0.49 ± 0.05	2.8 ± 0.4

[a] Values determined for WT PPase (Baykov et al., 1996) are shown in parentheses. [b] For pH 7.9.

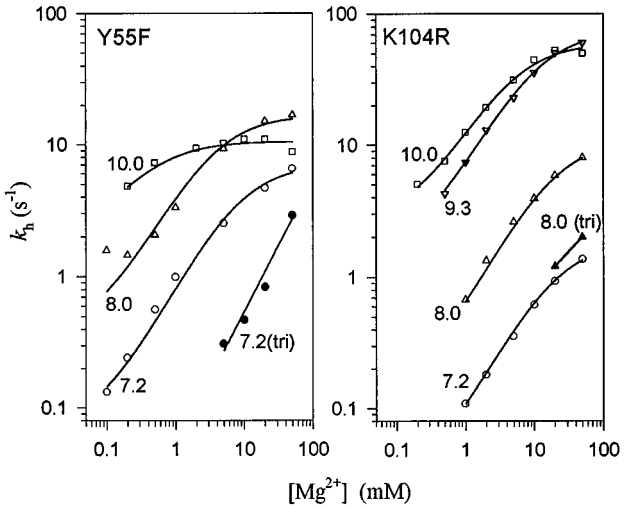

FIGURE 4: Dependencies of k_h on $[Mg^{2+}]$ at fixed pH values. Lines are drawn to eq 3 using parameter values shown in Table 3; the k_h data for trimeric Y55F PPase and K104R PPase were approximated by a straight line. Open symbols, hexameric enzymes; closed symbols, trimeric enzymes. Values of pH are shown on the curves.

shown by the shift of activity vs enzyme concentration profiles (Figure 2) to lower enzyme concentration (data not shown), as well as by the larger activity decreases on enzyme dilution seen at the lower temperature (Figure 3). The hexamers of the E20D, H136Q, and H140Q variants are also cold-destabilized (Velichko et al., 1995).

The reversibility of the temperature effects on enzyme activity (Figure 3) allowed estimation of rate parameters governing the hexamer−trimer equilibrium (Table 1). The dissociation constant, $K_d = k_d/k_a$, was derived from the activity vs enzyme concentration profiles (Figure 2) using eqs 1 and 2. As these values make clear, the hexamer stabilities for the two variant PPases are comparable at 25 °C. The decreased stability of Y55F relative to K104R variant at 0 °C is due solely to a difference in k_a values, suggesting that Y55F substitution induces a more pronounced conformational change in trimer at low temperature than does K104R substitution.

Mg^{2+} Binding. As measured by equilibrium dialysis, there are no significant changes in the dissociation constants (K_{m1} and K_{m2}) for Mg^{2+} binding to two tight sites at pH 7.2 and 8.0 and to three sites (K_{m1}, K_{m2}, and K_{m3}) at pH 9.3 in the Y55F and K104R variants as compared with WT PPase (Table 2).

Kinetics of PP_i Hydrolysis by Hexameric Enzymes. Values of k_h and $k_h/K_{m,h}$ for PP_i hydrolysis were measured for Y55F and K104R PPase as functions of pH and Mg^{2+} concentration (Figures 4 and 5). Values of k_h were fit to eq 3, which accounts simultaneously for the $[Mg^{2+}]$ and pH dependence of this parameter, yielding the pK_a values and binding

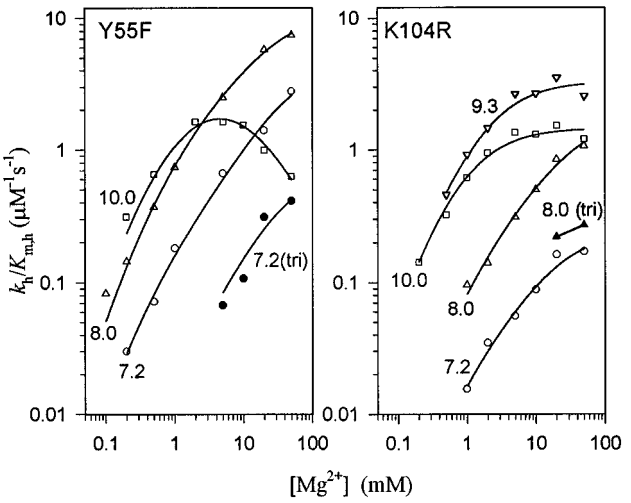

FIGURE 5: Dependencies of $k_h/K_{m,h}$ on $[Mg^{2+}]$ at fixed pH values. Open symbols, hexameric enzymes; closed symbols, trimeric enzymes. Values of pH are shown on the curves.

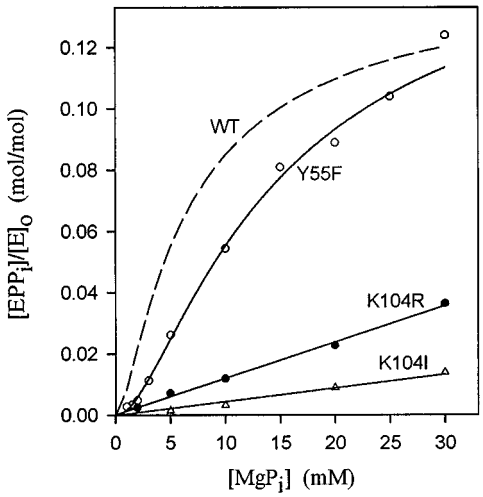

FIGURE 6: Formation of enzyme-bound PP_i by WT, Y55F, K104R, and K104I PPase at pH 7.2 in the presence of 20 mM Mg^{2+}. The lines shown for Y55F and WT PPase were drawn to eq 4; the corresponding parameter values for Y55F PPase were taken from Table 4 and for WT PPase (dashed line) from a previous work (Käpylä et al., 1995). The K104R and K104I PPase data were approximated by straight lines.

Table 3: Rate and Equilibrium Constants for Scheme 3[a]

	WT PPase[b]	Y55F PPase	K104R PPase
K^{H2}_{a3} (mM)	undetected	12 ± 3	20 ± 2
K^{H}_{a3} (mM)	>50	0.8 ± 0.3	8.5 ± 1.4
$k_h^{(3)}$ (s^{-1})	undetected	23 ± 4	130 ± 20
$k_h^{(2)}$ (s^{-1})	199 ± 8	2.0 ± 0.6	3.2 ± 0.4
pK'_{ESH2}	undetected	7.6 ± 0.2	9.0 ± 0.1
pK'_{ESH}	<9.2	9.9 ± 0.2	10.0 ± 0.1
pK_{ESH2}	6.7 ± 0.7	8.6 ± 0.2	9.4 ± 0.1

[a] Derived from initial velocity experiments. [b] Baykov et al. (1996); Volk et al. (1996).

constants shown in Table 3. The most noteworthy results are as follows: (a) For both variants, $k_h^{(2)}$ is reduced dramatically (~100-fold), whereas $k_h^{(3)}$ is much less affected, especially for K104R PPase (the value of $k_h^{(3)}$ for WT PPase is not known but is unlikely to exceed 200 s^{-1}; Baykov et al., 1996). (b) pK_a values for the essential basic group are markedly increased in both four- and five-Mg-containing complexes (making the reasonable assumption that, for WT PPase, $pK'_{ESH2} < pK_{ESH2}$)—a rise is also seen for the acidic pK_a of the five-Mg complex, although here the magnitude may be less than one unit. (c) Binding of the fifth metal ion to the enzyme−substrate complex (K^{H}_{a3}) is facilitated, especially in the Y55F PPase.

For K104I PPase, k_h was 0.2 s^{-1} at pH 8.0 and 20 mM Mg^{2+}; this variant was not characterized further kinetically.

Kinetics of PP_i Hydrolysis by Trimeric Enzymes. Through careful control of experimental conditions, it proved possible to measure k_h and $k_h/K_{m,h}$ values for the trimeric forms of both Y55F PPase and K104R PPase. For the values displayed in Figures 4 and 5, two lines of evidence rule out the possibility that the activities measured result from hexamer formation during the assay. First, hexamer formation is a slow reaction. For example, the association rate constant of 65 μM^{-1} h^{-1} measured for K104R PPase (Table 1) would correspond to a half-time of 1.5 h for hexamer formation at the 0.01 μM enzyme concentration used in the hydrolysis assay. The association rate constant is even lower for Y55F PPase (Table 1). Second, for both variants, measured k_h and $k_h/K_{m,h}$ values are considerably lower for trimer than for hexamer, yet the initial rates of product formation are strictly linear in all cases. Were hexamer being formed during the assay, a positive deviation from linearity would have been expected.

For Y55F PPase, values for k_h and $k_h/K_{m,h}$ were determined at pH 7.2. The k_h dependence showed no saturation with increasing Mg^{2+} concentration (Figure 4), implying that the value of k_h for trimer at saturating $[Mg^{2+}]$ is $\geq k_h$ for hexamer and that K_{a3}^{app} (the metal binding constant governing this dependence) >50 mM (for hexamer, $K_{a3}^{app} = 7 \pm 1$ mM). Thus, dissociation of Y55F PPase into trimers does not diminish the catalytic activity of the EM_3S complex (at least at pH 7.2), although it does increase substrate $K_{m,h}$ and weakens metal binding. The latter effects account for the apparent inactivation accompanying hexamer dissociation (Figures 2 and 3).

Trimeric K104R PPase exhibited an increased tendency to aggregate during the activity assay, resulting in markedly nonlinear product formation curves and limiting our ability to perform activity measurements. Two factors are responsible for this different behavior of K104R PPase vis-à-vis the Y55F variant: a higher k_a value (Table 1) and a lower k_h value (Figure 4), resulting in higher enzyme concentrations in the assays. The latter factor was particularly problematic at low Mg^{2+} concentration. The limited data available for trimeric K104R PPase at pH 8.0 (Figures 4 and 5) suggest that dissociation into trimers affects the catalytic properties of the two variants in a similar manner.

Microscopic Rate Constants for Hexameric Enzyme Catalysis of PP_i-P_i Equilibration. We previously determined all rate constants in Scheme 1 for WT PPase at pH 6.5−9.3 (Käpylä et al., 1995; Baykov et al., 1996) by measuring steady-state rates of PP_i hydrolysis, PP_i synthesis, and P_i-H_2O oxygen exchange and equilibrium EPP_i formation at saturating concentrations of the respective substrates. MgP_i binding is weakened in the variant PPases (Figure 6), making it more difficult (Y55F PPase) or even impracticable (K104R PPase) to extrapolate measured values to saturating MgP_i concentration. As a result, estimates of k_1-k_8 were only made for Y55F PPase and only at higher $[Mg^{2+}]$; 10−50 mM at pH 7.2, 10−20 mM at pH 8.0. In making these estimates, values of K_3, K_5, and K_7 were obtained from the

Table 4: Rate and Equilibrium Constants for WT and Y55F PPase

parameter	WT PPase[a]		Y55F PPase				
			pH 7.2			pH 8.0	
	pH 7.2, 20 mM Mg^{2+}	pH 8.0, 20 mM Mg^{2+}	50 mM Mg^{2+}	20 mM Mg^{2+}	10 mM Mg^{2+}	20 mM Mg^{2+}	10 mM Mg^{2+}
k_h (s^{-1})	155 ± 8	187 ± 5	6.6 ± 0.1	4.7 ± 0.4	4.0 ± 0.2	15 ± 1	12 ± 1
$k_{h/Km,h}$ (μM^{-1} s^{-1})	44 ± 8	55 ± 5	2.8 ± 0.1	1.4 ± 0.2	0.94 ± 0.09	5.8 ± 0.6	4.0 ± 0.3
K_3	5.8 ± 0.5	6 ± 3	5.0 ± 0.9	4.8 ± 0.8	5.0 ± 1.4	4.9 ± 1.1	5.0 ± 1.3
K_5 (mM)	7.4 ± 1.2	13 ± 7	12 ± 4	16 ± 7	14 ± 4	19 ± 8	24 ± 7
K_7 (mM)	1.6 ± 0.2	0.49 ± 0.14	6 ± 4	6 ± 5	14 ± 8	2± 1	4 ± 3
k_1 (μM^{-1} s^{-1})	46 ± 5	56 ± 4	4.7 ± 1.1	2.1 ± 0.5	1.2 ± 0.2	6.7 ± 0.9	4.7 ± 0.5
k_2 (s^{-1})	20 ± 5 (12 ± 3)[b]	11 ± 9	8.3−14.9	6.8−10.7	4.8−6.4	7.9−9.0	7.8−9.0
k_3 (s^{-1})	800 ± 180	800 ± 400	19 ± 3	18 ± 1	19 ± 2	62 ± 2	59 ± 3
k_4 (s^{-1})	140 ± 30	130 ± 20	3.8 ± 1.3	3.8 ± 0.8	3.8 ± 1.5	13 ± 3	12 ± 4
k_5 (s^{-1})	440 ± 110	500 ± 140	50 ± 20	50 ± 20	60 ± 20	80 ± 20	65 ± 23
k_6 (mM^{-1} s^{-1})	59 ± 17	38 ± 22	4 ± 3	3 ± 2	4 ± 3	4 ± 3	3 ± 2
k_7 (s^{-1})	400 ± 100	600 ± 300	14 ± 4	7.5 ± 1.6	5.7 ± 0.9	29 ± 8	21 ± 7
k_8 (mM^{-1} s^{-1})	260 ± 70	1100 ± 700	2.4 ± 1.3	1.2 ± 0.7	0.4 ± 0.2	13 ± 6	5 ± 2.5

[a] Käpylä et al. (1995). [b] Baykov et al. (1990).

Table 5: Estimation of k_1, k_2, and k_3 from Oxygen Exchange and PP_i Synthesis Data[a]

pH	$[Mg^{2+}]$ (mM)	$[MgP_i]$ (mM)	f_{epp} (mol/mol)	$v_{ex}/[E]_t$ (s^{-1})	P_c	$v_s/[E]_t$ (s^{-1})	k_1[b] ($\mu M^{-1}s^{-1}$)	k_2[c] (s^{-1})	k_3[d] (s^{-1})
				Y55F PPase					
7.2	50	20	0.120 ± 0.010	2.22 ± 0.13	0.077 ± 0.003	1.00 ± 0.09	4.6 ± 0.7	8.3−14.9	19 ± 3
7.2	20	20	0.089 ± 0.004	1.60 ± 0.02	0.068 ± 0.005	0.60 ± 0.04	2.2 ± 0.5	6.8−10.7	18 ± 1
7.2	10	20	0.079 ± 0.006	1.47 ± 0.02	0.062 ± 0.002	0.38 ± 0.02		4.8−6.4	19 ± 2
7.2	5	20	0.078 ± 0.008	0.98 ± 0.15	0.059 ± 0.003	0.27 ± 0.03	0.88 ± 0.11	3.5−4.7	13 ± 3
8	20	10	0.071 ± 0.002	4.23 ± 0.04	0.139 ± 0.005	0.56 ± 0.07	6.7 ± 0.8	7.9−9.0	62 ± 2
8	10	10	0.067 ± 0.003	3.77 ± 0.04	0.154 ± 0.007	0.52 ± 0.07		7.8−9.0	59 ± 3
8	5	10	0.067 ± 0.004	3.70 ± 0.10	0.142 ± 0.008	0.38 ± 0.01	2.8 ± 0.2	5.7−6.3	57 ± 5
8	2	10	0.097 ± 0.002	3.22 ± 0.06	0.155 ± 0.007	0.29 ± 0.01		3.0−3.3	35 ± 1
8	1	10	0.094 ± 0.004						
8	0.5	10	0.093 ± 0.003						
				K104R PPase					
7.2	50	20	0.0212 ± 0.003	0.121 ± 0.002	0.058 ± 0.001	0.036 ± 0.002	0.24 ± 0.02	1.7−2.4	5.8 ± 0.9
7.2	20	20	0.0228 ± 0.002	0.104 ± 0.002	0.056 ± 0.003	0.028 ± 0.002	0.22 ± 0.02	1.2−1.7	4.6 ± 0.5
7.2	10	20	0.0198 ± 0.001	0.088 ± 0.005	0.049 ± 0.004	0.022 ± 0.001	0.12 ± 0.01	1.1−1.5	4.5 ± 0.5
7.2	5	20	0.0268 ± 0.002	0.060 ± 0.006	0.045 ± 0.006	0.022 ± 0.001	0.08 ± 0.01	0.8−1.2	2.3 ± 0.3
8	20	10	0.0066 ± 0.0004	0.150 ± 0.003	0.059 ± 0.006	0.031 ± 0.003	1.1 ± 0.1	4.7−5.9	23 ± 2
8	10	10	0.0067 ± 0.0002	0.148 ± 0.008	0.059 ± 0.002	0.035 ± 0.002	0.6 ± 0.1	5.2−6.8	22 ± 2
8	5	10	0.0070 ± 0.0008	0.151 ± 0.004	0.063 ± 0.004	0.038 ± 0.002	0.41 ± 0.04	5.4−7.2	22 ± 3
8	2	10	0.0107 ± 0.0004	0.114 ± 0.003	0.066 ± 0.002	0.035 ± 0.001	0.19 ± 0.02	3.3−4.7	11 ± 1
8	1	10	0.0132 ± 0.0010	0.078 ± 0.004	0.063 ± 0.006	0.032 ± 0.004	0.15 ± 0.02	2.4−4.1	6.0 ± 0.8
8	0.5	10	0.0235 ± 0.0015	0.029 ± 0.006	0.049 ± 0.015	0.024 ± 0.002		1.0−5.6	1.3 ± 0.4
8	0	100[e]	< 0.001						

[a] Measured values represent means of 2−4 independent determinations ± mean deviation. [b] Estimated with eq 15. [c] Estimated with eq 14. [d] Estimated with eq 13. [e] Free P_i concentration.

dependence of f_{epp} on $[MgP_i]$ (Figure 6). These values were combined with the values of k_h, $k_h/K_{m,h}$, k_2, k_3, and P_c to yield all eight rate constants (Springs et al., 1981; Smirnova et al., 1995).

The estimates of k_1-k_8 (Table 4), demonstrate that, over the range of $[Mg^{2+}]$ and pH employed, k_3, k_4, k_5, and k_6 are largely independent of $[Mg^{2+}]$, whereas k_1, k_7, and k_8 increase with increasing $[Mg^{2+}]$. Furthermore, k_1, k_3, k_4, k_7, and k_8 rise significantly (>3-fold) on raising pH from 7.2 to 8.0, whereas k_2, k_5, and k_6 change little if at all. An interesting consequence of the changes with $[Mg^{2+}]$ at pH 7.2 is that whereas both k_3 and k_7 are partially rate-determining for k_h at high (50 mM) Mg^{2+}, at low (10 mM) Mg^{2+} k_7 is almost exclusively rate-determining.

Values of f_{epp}, v_s, and v_{ex} were used with eqs 13−15 to estimate values for k_1-k_3 for both Y55F- and K104R PPase at pH 7.2 and 8.0 over wide ranges of $[Mg^{2+}]$. These values, summarized in Table 5, demonstrate several prominent differences with respect to WT PPase. First, values of f_{epp} show a tendency to decrease rather than increase (Baykov et al., 1990) with increasing $[Mg^{2+}]$. This effect is most pronounced with K104R PPase at pH 8.0. Second, values of P_c are, in general, smaller than the value of 0.16−0.24 determined for WT PPase (Baykov et al., 1990; Käpylä et al., 1995), and for Y55F PPase, P_c increases with pH, while for WT PPase, it is constant at pH 6.5−8.0 and decreases above pH 8.5 (Baykov et al., 1996). Third, values of k_3 measured at saturating Mg^{2+} concentration are significantly (3−4-fold) greater at pH 8.0 than at pH 7.2; for WT PPase, k_3 is fairly constant in the pH range 6.5−9.3 (Baykov et al., 1996). Fourth, for both variants substrate is bound more rapidly at high Mg^{2+} concentration, where EMg_3 predominates (Table 2), in contrast to WT PPase, for which EMg_2 binds substrate most rapidly (Baykov et al., 1996). Fifth, k_1 values are lower for both variants by 1−3 orders of magnitude, compared to WT PPase (Baykov et al., 1996). The important similarities with WT PPase include the invariance of P_c with $[Mg^{2+}]$ and the magnitude of the values of k_2 and v_s.

Interestingly, K104I PPase, while having only 0.1% of the hydrolytic activity of WT PPase, exhibited appreciable EPP_i formation (11% vs WT PPase at 30 mM MgP_i) (Figure 6).

DISCUSSION

Role of Tyr55 and Lys104 in Quaternary Structure Stabilization. Tyr55 and Lys104 form a hydrogen bond in the crystal structure of E-PPase complexed with Mg^{2+} (Figure 1), which occupies a central position in the hydrogen-bonding network in the active site (Kankare et al., 1996a,b). The three variants studied in this work either eliminate this hydrogen bond by deletion of the hydroxyl (Y55F) or the amino (K104I) group or would be expected to modify it by substituting a guanidino for the amino group (K104R).

Our earlier work on the E20D variant (Volk et al., 1996) demonstrated a linkage between the hydrogen-bonding network in the active site and the trimer−trimer interaction, which is reinforced by the results of the present studies. This linkage is clearly mediated by conformational change since no active-site residues participate directly in the subunit interface. Of the two residues under study, Tyr55 and Lys104, the former is clearly more important for hexamer stability. Though both Y55F and K104I substitutions eliminate the hydrogen bond between Tyr55 and Lys104, only the former destabilizes the hexamer. In the K104I variant, Tyr55 may form a hydrogen bond with Asp70. Such an interaction exists in the apoenzyme structure (Kankare et al., 1996b) and may help to position the phenolic ring of Tyr55 in a hydrophobic cluster with Phe137 and Phe138 [Figure 5 of Kankare et al. (1996a)]. The latter residues are found in α-helix A, which also contains His136 and His140, the key residues in the trimer−trimer interface (Baykov et al., 1995). The decreased stability of hexameric K104R PPase may reflect a change in the position of Tyr55 resulting from interaction with the substituted guanidino group. Interestingly, the effects of the Y55F and K104R substitutions on hexamer stability (K_d) are similar at 25 °C and different at 0 °C (Table 1).

The k_h value for trimeric Y55F PPase, and possibly for K104R PPase as well, appears to be at least as large as that for the hexameric form, but the trimeric form exhibits decreased $k_h/K_{m,h}$ values and weakened Mg^{2+} binding. In these respects, trimeric Y55F- (and K104R-) PPase(s) resemble the trimeric PPase obtained by substitutions of His136 and His140 in the subunit interface (Baykov et al., 1995) and differ from trimeric E20D-PPase, which is nearly inactive (Volk et al., 1996).

Role of Tyr55 and Lys104 in Catalysis. Relative to WT PPase, both Y55F and K104R variants are characterized by markedly increased pK_a values for the essential base and an increased pK_a for the essential acid (Table 3). In addition, both variants require a Mg^{2+} stoichiometry of 5 in the enzyme−substrate complex ($k_h^{(2)} << k_h^{(3)}$; k_1 for EMg_2 << k_1 for EMg_3), as opposed to WT PPase, where the dominant hydrolysis route is via the complex containing four Mg^{2+} ions (Baykov et al., 1996). These two effects are common for a number of active-site variants of E-PPase (Salminen et al., 1995; Käpylä et al., 1995; Volk et al., 1996), which we attribute to the highly integrated nature of active-site structure. Binding of the fifth metal ion allows at least partial recovery from various distortions resulting from active-site substitutions and may reflect a tightening of the active site following such binding.

A more specific effect of K104R substitution on substrate and product binding is evident from the large decrease in the value of k_1 (50−200-fold measured at 20 mM Mg^{2+}; Tables 4 and 5) for this variant as well as the much weakened binding of MgP_i, as indicated by the linearity of the plots for enzyme-bound PP_i formation up to 30 mM MgP_i (Figure 6). This most likely reflects an effect on binding to the lower affinity P2 site, based on recent results of Hyytiä et al. (manuscript in preparation) showing this mutation to have little effect on P1 site binding. This conclusion is also in accord with the crystal structure of the *S. cerevisiae* PPase−$Mn_4(P_i)_2$ complex (Heikinheimo et al., 1996), in which Lys154, equivalent to Lys104 in E-PPase, forms a tight hydrogen bond to Asp120, which in turn binds directly to M1 and M2. The K104R substitution, though having only minor effects on K_{m1}, K_{m2}, or K_{m3} (Table 2), evidently distorts the interaction of M1 and M2 with subsite P2 (Figure 1). Neither M1 nor M2 has a direct interaction with subsite P1.

Tyr93 in *S. cerevisiae* PPase, which is equivalent to Tyr55 in E-PPase, has a hydrogen bond to P2 (Figure 1). Y55F substitution also decreases k_1 and weakens MgP_i binding (Tables 4 and 5). However, the effects are less marked than for K104R substitution, suggesting that the loss of the Tyr55 hydrogen bond to P2 and to Lys104 is less critical for overall active-site structure. Although Tyr55 is responsible for large changes in E-PPase absorption spectrum upon Mg^{2+} binding (Avaeva et al., 1995), the data in Table 2 indicate that this effect is not due to coordination of Mg^{2+} to Tyr55 hydroxyl. Nor is such an interaction with Tyr93 seen in the crystal structure of the *S. cerevisiae* PPase−$Mn_4(P_i)_2$ complex (Heikinheimo et al., 1996; Harutyunyan et al., 1996a).

As measured at 20 mM Mg^{2+} at either pH 7.2 or 8.0, k_3, the rate constant for hydrolysis of enzyme-bound PP_i, is considerably reduced in both variants relative to wild-type enzyme. The factors at pH 7.2, 40- and 160-fold for the Y55F and K104R variants, respectively, are decreased to 13- and 35-fold at pH 8.0, due to the rise in k_3 values for both variants over this pH range, which contrasts with the invariant value for WT PPase. The rise in the variant k_3 values with increased pH, which is seen over a wide range of [Mg^{2+}], is similar to what was found earlier for D97E PPase at a single [Mg^{2+}] of 20 mM (Käpylä et al., 1995) and provides strong support for an essential base modulating the value of k_3. The values in Table 5 allow calculation of approximate values for the pK_a of this base of 7.9 (Y55F) and >8.3 (K104R) and for the pH-independent values of k_3 of 110 s^{-1} (Y55F) and >70 s^{-1} (K104R). We assume that an essential base also modulates the value of k_3 for WT PPase and interpret the result (Käpylä et al., 1995; Baykov et al., 1996) that k_3 for WT PPase varies little between pH 6.5 and 9.3 as indicating that the essential base pK_a for it is <6.5. The pH-independent value for k_3 for WT PPase is ∼800 s^{-1} (Table 4). Thus the large factors seen for k_3 at pH 7.2 comparing WT PPase and its variants reflect significant effects on both the essential base pK_a and the pH-independent value for k_3.

In a recent paper (Heikinheimo et al., 1996), we presented structural evidence that a water molecule/hydroxide ion bridges M1 and M2. We also summarized our previous results (Salminen et al., 1995; Käpylä et al., 1995) showing that it is probably the essential base for hydrolysis of enzyme-bound PP_i. Modeling further indicated (Heikinheimo et al., 1996) that the OH^- may directly attack the PP_i. Our current

results indicate that the Y55F and K104R substitutions distort the active site sufficiently both to weaken M1 and M2 interaction with the bridging water (thus raising its pK_a) and to decrease the intrinsic catalytic power of the enzyme, as measured by the pH-independent value of k_3.

In summary, we have shown that two relatively conservative substitutions, Y55F and K104R, at the PPase active site strongly affect both the quaternary structure of the enzyme as well as several rate (k_1, k_3, and k_4) and equilibrium (K_1, K_5 and/or K_7, essential base pK_a) parameters. These effects reflect distortions arising from substitution that propagate through the tightly integrated active site and reach as far as the trimer−trimer interface. The binding of a fifth Mg^{2+} per enzyme subunit apparently compensates for these distortions, but only partially.

ACKNOWLEDGMENT

We thank P. V. Kalmykov and N. N. Magretova for their help in this work.

REFERENCES

Avaeva, S. M., Rodina, E. V., Kurilova, S. A., Nazarova, T. I., Vorobjeva, N. N., Harutyunyan, E. H., & Oganessyan, V. Yu. (1995) *FEBS Lett. 377*, 44−46.

Baltscheffsky, M., & Baltscheffsky, H. (1992) in *Molecular Mechanisms in Bioenergetics* (Ernster, L., Ed.) pp 331−348, Elsevier, Amsterdam.

Baykov, A. A., Dudarenkov, V. Yu., Käpylä, J., Salminen, T., Hyytiä, T., Kasho, V. N., Husgafvel, S., Cooperman, B. S., Goldman, A., & Lahti, R. (1995) *J. Biol. Chem. 270*, 30804−30812.

Baykov, A. A., Hyytiä, T., Volk, S. E., Kasho, V. N., Vener, A. V., Goldman, A., Lahti, R., & Cooperman, B. S. (1996) *Biochemistry 35*, 4655−4661.

Baykov, A. A., Shestakov, A. S., Kasho, V. N., Vener, A. V., & Ivanov, A. H. (1990) *Eur. J. Biochem. 194*, 879−887.

Chen, J., Brevet, A., Formant, M., Leveque, F., Schmitter, J.-M., Blanquet, S., & Plateau, P. (1990) *J. Bacteriol. 172*, 5686−5689.

Cooperman, B. S., Baykov, A. A., & Lahti, R. (1992) *Trends Biochem. Sci. 17*, 262−266.

Gonzalez, M. A., Webb, M. R., Welsh, K. M., & Cooperman, B. S. (1984) *Biochemistry 23*, 797−801.

Hackney, D. D., & Boyer, P. D. (1978) *Proc. Natl. Acad. Sci. U.S.A. 75*, 3133−3137.

Harutyunyan, E. H., Kuranova, I. P., Vainshtein, B. K., Höhne, W. E., Lamzin, V. S., Dauter, Z., Teplyakov, A. V., & Wilson, K. S. (1996a) *Eur. J. Biochem. 239*, 220−228.

Harutyunyan, E. H., Oganessyan, V. Yu., Oganessyan, N. N., Terzyan, S. S., Popov, A. N., Rubinskiy, S. B., Vainstein, B. K., Nazarova, T. I., Kurilova, S. A., Vorobjeva, N. N., & Avaeva, S. M. (1996b) *Kristallografiya 41*, 84−96.

Heikinheimo, P., Lehtonen, J., Baykov, A. A., Lahti, R., Cooperman, B. S., & Goldman, A. (1996) *Structure 4*, 1491−1508.

Josse, J. (1966) *J. Biol. Chem. 241*, 1938−1947.

Kankare, J., Salminen, T., Lahti, R., Cooperman, B., Baykov, A. A., & Goldman, A. (1996a) *Acta Crystallogr. D 52*, 551−563.

Kankare, J., Salminen, T., Lahti, R., Cooperman, B., Baykov, A. A., & Goldman, A. (1996b) *Biochemistry 35*, 4670−4677.

Käpylä, J., Hyytiä, T., Lahti, R., Goldman, A., Baykov, A. A., & Cooperman, B. S. (1995) *Biochemistry 34*, 792−800.

Kornberg, A. (1982) in *Horizons in Biochemistry* (Kasha, H., & Pullman, P., Eds.) pp 251−264, Academic Press, New York.

Lahti, R., Pohjanoksa, K., Pitkäranta, T., Heikinheimo, P., Salminen, T., Meyer, P., & Heinonen, J. (1990a) *Biochemistry 29*, 5761−5766.

Lahti, R., Salminen, T., Latonen, S., Heikinheimo, P., Pohjanoksa, K., & Heinonen, J. (1990b) *Eur. J. Biochem. 198*, 293−297.

Lundin, M., Baltscheffsky, H., & Ronne, H. (1991) *J. Biol. Chem. 266*, 12168−12172.

Nyrén, P., & Lundin, A. (1985) *Anal. Biochem. 151*, 504−509.

Rea, P. A., & Poole, R. J. (1993) *Annu. Rev. Plant Physiol. Plant Mol. Biol. 44*, 157−180.

Salminen, T., Käpylä, J., Heikinheimo, P., Kankare, J., Goldman, A., Heinonen, J., Baykov, A. A., Cooperman, B. S., & Lahti, R. (1995) *Biochemistry 34*, 782−791.

Smirnova, I. N., Kasho, V. N., Volk, S. E., Ivanov, A. H., & Baykov, A. A. (1995) *Arch. Biochem. Biophys. 318*, 340−348.

Sonnewald, U. (1992) *Plant J. 2*, 571−581.

Springs, B., Welsh, K. M., & Cooperman, B. S. (1981) *Biochemistry 20*, 6384−6391.

Teplyakov, A., Obmolova, G., Wilson, K. S., Ishii, K., Kaji, H., Samejima, T., & Kuranova, I. (1994) *Protein Sci. 3*, 1098−1107.

Velichko, I. S., Volk, S. E., Dudarenkov, V. Yu., Magretova, N. N., Chernyak, V. Ya., Goldman, A., Cooperman, B. S., Lahti, R., & Baykov, A. A. (1995) *FEBS Lett. 359*, 20−22.

Volk, S. E., Dudarenkov, V. Yu., Käpylä, J., Kasho, V. N., Voloshina, O. A., Salminen, T., Goldman, A., Lahti, R., Baykov, A. A., & Cooperman, B. S. (1996) *Biochemistry 35*, 4662−4669.

Wong, S. C. K., Hall, D. C., & Josse, J. (1970) *J. Biol. Chem. 245*, 4335−5345.

BI9629844